Reversibility and Hierarchy of Thermal Transition of Hen Egg-White Lysozyme Studied by Small-Angle X-Ray Scattering

Shigeki Arai and Mitsuhiro Hirai
Department of Physics, Gunma University, Maebashi 371-8510, Japan

ABSTRACT To clarify mechanisms of folding and unfolding of proteins, many studies of thermal denaturation of proteins have been carried out at low protein concentrations because in many cases thermal denaturation accompanies a great tendency of aggregation. As small-angle x-ray scattering (SAXS) measurements are liable to use low-concentration solutions of proteins to avoid aggregation, SAXS has been regarded as very difficult to observe detailed features of thermal structural transitions such as intramolecular structural changes. By using synchrotron radiation SAXS, we have found that the presence of repulsive interparticle interaction between proteins can maintain solute particles separately to prevent further aggregation in thermal denaturation processes and that under such conditions the thermal structural transition of hen egg-white lysozyme (HEWL) holds high reversibility even at 5% w/v HEWL below pH ~5. Because of the use of the high concentration of the solutions, the scattering data has enough high-statistical accuracy to discuss the thermal structural transition depending on the structural hierarchy. Thus, the tertiary structural change of HEWL starts from mostly the onset temperature determined by the differential scanning calorimetry measurement, which accompanies a large heat absorption, whereas the intramolecular structural change, corresponding to the interdomain correlation and polypeptide chain arrangement, starts much prior to the above main transition. The present finding of the reversible thermal structural transitions at the high protein concentration is expected to enable us to analyze multiplicity of folding and unfolding processes of proteins in thermal structural transitions.

INTRODUCTION

Many calorimetric studies were carried out to clarify the thermodynamic basis of the stability of the conformational states of proteins (Tanford, 1968, 1970; Pfeil and Privalov, 1976a,b,c), and now it is widely considered that under equilibrium conditions the thermal transitions of single-domain proteins in solutions are usually two-state where only the fully folded and unfolded states are populated (Privalov and Gill, 1988; Privalov, 1989). Calorimetric studies suggested that hen egg-white lysozyme (HEWL) is a typical protein showing a cooperative two-state thermal transition without an intermediate state, whereas hydrogen exchange experiments using two-dimensional nuclear magnetic resonance (NMR) have suggested that HEWL consists of the two structural domains that differ significantly in the folding pathway and that these different parts are expected to be stabilized with very different kinetics (Miranker et al., 1991; Radford et al., 1992a,b; Buck et al., 1993).

Despite these results, the x-ray scattering method, which is known to provide direct information about the solute particle structure, has been rarely applied to the thermal structural transition studies of proteins in comparison with folding and unfolding studies of proteins under the presence of various denaturants (Kataoka et al., 1995). As x-ray scattering studies of protein structures in solutions need relatively high-concentration samples in comparison with other spectroscopic studies, such as circular dichroism, it is usually very difficult to determine degree of thermal transition of both tertiary and intramolecular structures of proteins by using x-ray scattering because of a great tendency of aggregation. To suppress such an aggregation effect in the denaturation processes, in many cases x-ray scattering experiments are carried out by reducing protein concentrations as low as possible, and an extrapolation method using the Zimm plot is used (Kataoka et al., 1995; Kataoka and Goto, 1996). However, this method done by lowering solute concentration is applicable only to scattering data restricted in a very small-angle region with relatively high statistical accuracy, which gives us only structural information such as gyration radius. Therefore, we tend to discard an intramolecular structural information obtained from wide-angle scattering data owing to very low statistics.

By the way, under the conditions far from an isoelectric point, proteins exist in solutions as positively or negatively changed macro-ions, such as ionic micelles (Hirai et al., 1996a,b). To conquer the above conflicting demand for x-ray scattering studies of thermal structural transitions of proteins, namely, to obtain wide-angle scattering data with high-statistical accuracy under unaggregative conditions, the repulsive interactions between proteins through Coulomb potential can be positively used to prevent some aggregation. By using the synchrotron radiation small-angle x-ray scattering (SR-SAXS) method we have successfully observed the highly reversible thermal structural transition of HEWL even at high concentration. The present finding will provide us with a new aspect of the intramolecular structural transition of protein in the unfolding and folding process under heating and cooling.

Received for publication 17 December 1997 and in final form 20 January 1999.

Address reprint requests to Prof. Mitsuhiro Hirai, Department of Physics, Gunma University, 4-2 Aramaki, Maebashi 371-8510, Japan. Tel.: 81-272-20-7554; Fax: 81-272-20-7551; E-mail: hirai@sun.aramaki.gunma-u.ac.jp.

0006-3495/99/04/2192/06 $2.00

MATERIALS AND METHODS

Samples

The protein used was HEWL, three times crystallized, purchased from Sigma Chemical Co. (St. Louis, MO). As a repulsive interparticle interaction between proteins is greatly weakened by the electric-shielding effect of the presence of counterions surrounding the protein, we solubilized lysozyme in water for which the pH had been adjusted only by adding HCl before solubilization. Final pH values of the solutions were determined to be 2.8, 4.8, and 7.2 by using a digital pH meter HM-60V from TOA Electronics Ltd. For the SAXS experiments, the concentration of the lysozyme solution was varied from 0.5% w/v to 20% w/v. The concentration of the samples used for the temperature dependence measurements were 5% w/v.

Small-angle x-ray scattering measurements

X-ray scattering experiments were carried out with a small-angle scattering spectrometer (Ueki et al., 1985) installed at the 2.5 GeV storage ring in the Photon Factory, Tsukuba, Japan. A one-dimensional position-sensitive proportional counter detected the scattering intensity. The wavelength used was 1.49 Å, and the sample-to-detector distance was 60 cm. A sample cell composed of a pair of mica windows with 1-mm path length contained the lysozyme solution, which was placed in a thermostatted cell holder with a precision below 0.1°C. The sample solution was heated stepwise from 20°C to 80°C with the temperature interval of 5°C. After the first heating, the sample solution was immediately cooled to 20°C and kept at this temperature for 1 h, when the second heating was started. The temperature of the samples was monitored by using a thermocouple device attached directly to the sample cell. The exposure time for one-shot measurement was 4 min, and the integrated exposure time for one sample was 52 min.

Differential scanning calorimetry measurements

The differential scanning calorimetry (DSC) measurements were done by using a differential scanning calorimeter PC DSC7 from Perkin Elmer Co. To compare SAXS data with DSC data directly, the samples of the DSC measurements were prepared in the same way used for the protein solutions in the scattering measurements (5% w/v). Scanning rate was 3°C/min in the temperature range from 10°C to 80°C. After the first heating, the sample was cooled to 10°C and kept at this temperature for 1 h when the second heating measurement was started.

Scattering data analysis

The following analyses were done. The distance distribution function $p(r)$ was calculated by the Fourier inversion of the scattering curve $I(q)$ as

$$p(r) = \frac{2}{\pi}\int_0^\infty rqI(q)\sin(rq)dq, \tag{1}$$

where q is the magnitude of scattering vector defined by $q = (4\pi/\lambda)\sin(\theta/2)$ (θ, the scattering angle; λ, the wavelength). The $p(r)$ function reflects the particle shape, the intraparticle scattering density distribution, and the interparticle correlation (Glatter, 1982). The maximal diameter D_{max} of the particle was estimated from the $p(r)$ function satisfying the condition $p(r) = 0$ for $r > D_{max}$. To reduce the Fourier truncation effect on the calculation of the $p(r)$ function, the extrapolation of the small-angle data sets by using the least-squares method for the Guinier plot ($\ln(I(q))$ vs. q^2) and the modification of the scattering intensity as

$$I'(q) = I(q)\exp(-kq^2) \tag{2}$$

(k is the artificial damping factor) were employed. As the use of the Guinier approximation for the determination of gyration radius R_g is known to lead to inherent systematic errors and similar difficulties caused by concentration or aggregation effect, we used the following equations (Glatter, 1982) to reduce such artifacts for the estimation of R_g:

$$I_{total} = \int_0^{D_{max}} p(r)dr \tag{3}$$

and

$$R_g^2 = \frac{\int_0^{D_{max}} p(r)r^2dr}{2\int_0^{D_{max}} p(r)dr} \tag{4}$$

Equation 3 was used for normalization of the $p(r)$ functions.

RESULTS AND DISCUSSION

Fig. 1 shows the concentration dependence of the scattering curve $I(q)$ of the lysozyme solution at pH 7.0 in 50 mM Hepes buffer as the concentration was varied from 0.5% w/v to 20% w/v. The abrupt decrease of the scattering intensity below $q \approx 0.02$ Å^{-1} results from the beam stopper. As is well known, the scattering curve $I(q)$ contains the structural information with different real-space distance depending on the observed q range. In the present case the broad peak at $q \approx 0.07$ Å^{-1} is evidently attributable to the interparticle correlation under repulsive Coulomb potential, whose width and height depend on the effective charge of the protein surface (Hirai et al., 1996a). Except for a highly concentrated system composed of large anisotropic-shaped particles forming liquid crystal ordering (Hirai et al., 1995, 1997), for globular particle systems in solutions the repulsive interaction between the particles usually produces only a broad single peak at the small q region owing to a large thermal energy of Brownian motion, which scarcely affects the scattering curve in the q region above the peak position

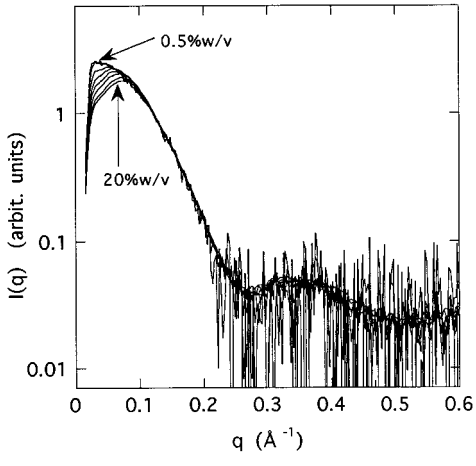

FIGURE 1 Concentration dependence of the scattering curve $I(q)$ of the HEWL solution in 50 mM Hepes buffer at 25°C. The concentration was varied from 0.5% w/v to 20% w/v. The scattering curves were normalized by the concentrations.

(Hirai et al., 1996a). Fig. 1 clearly shows such a situation. Thus, the scattering curve $I(q)$ in the q range of 0.1–0.2 $Å^{-1}$ mostly reflects the tertiary structure of lysozyme in the real space distance of ~30–60 Å, such as molecular shape and dimension, and the $I(q)$ in the q range of 0.3–0.6 $Å^{-1}$ mostly reflects the intramolecular structure in the real space distance of ~10–20 Å, such as structural domain correlation and polypeptide arrangement.

Fig. 2 shows the temperature dependence of the scattering curves $I(q)$ of the lysozyme solutions at different pH, where *A–C* correspond to pH 7.2, pH 4.8, and pH 2.8, respectively. For all solutions the change of the scattering curve in the q range of 0.3–0.6 $Å^{-1}$ starts gradually from 20°C. On the other hand, the change of the scattering curve in the q range of 0.1–0.2 $Å^{-1}$ starts from a higher temperature that depends on pH. This shows that with elevating temperature the intramolecular structural fluctuation or rearrangement starts prior to the major change of the tertiary structure. The above changing tendency is also indicated by the Kratky plots ($q^2I(q)$ vs. q) shown in Fig. 3. As is well known, the Kratky plot reflects the short-range interactions acting along the polymer chain from neighbor to neighbor, such as bond forces and hindrance of rotation, and also shows a certain rigidity of polymer chains (Kratky and Porod, 1949; Kriste, 1967; Kriste and Oberthür, 1982; Hirai et al., 1993, 1994). In Fig. 3 the temperature dependence of the Kratky plot in the q range of 0.4–0.6 $Å^{-1}$ well indicates that the gradual change of the intramolecular structure starts from 20°C, namely, that the polypeptide chain changes its conformation from a persistent chain with a rigid persistent curvature to a persistent chain with less persistent curvature (Kriste and Oberthür, 1982; Hirai et al., 1993, 1994). The broad peak at $q \approx 0.12$ $Å^{-1}$ in the Kratky plot, which is different from the interparticle correlation peak in Figs. 1 and 2, shows that the

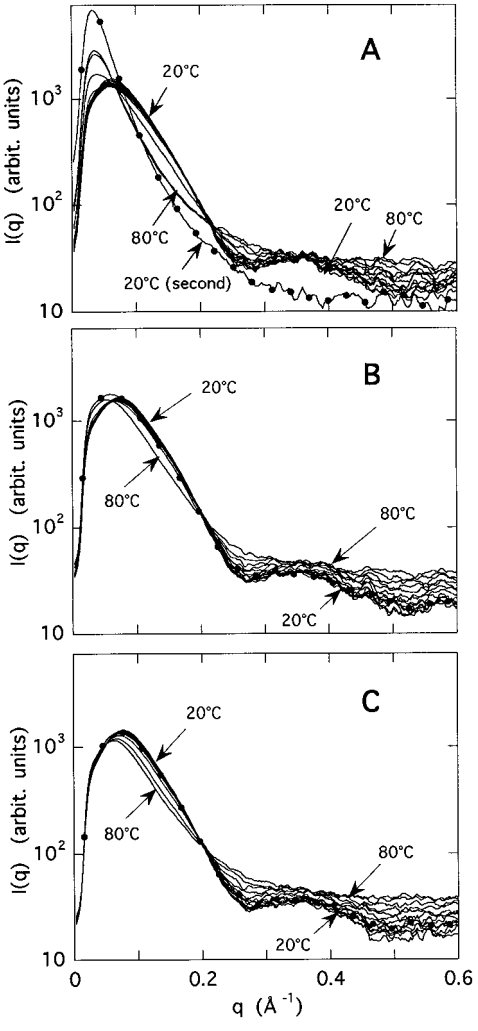

FIGURE 2 Temperature dependence of the scattering curves $I(q)$ of the HEWL solutions (5% w/v) at different pH values. (*A*) pH 7.2; (*B*) pH 4.8; (*C*) pH 2.8. The temperature was elevated stepwise from 20°C to 80°C with the temperature interval of 5°C. The solid lines with ● correspond to the lysozyme solutions that were cooled to 20°C after the first heating and kept at this temperature for 1 hour.

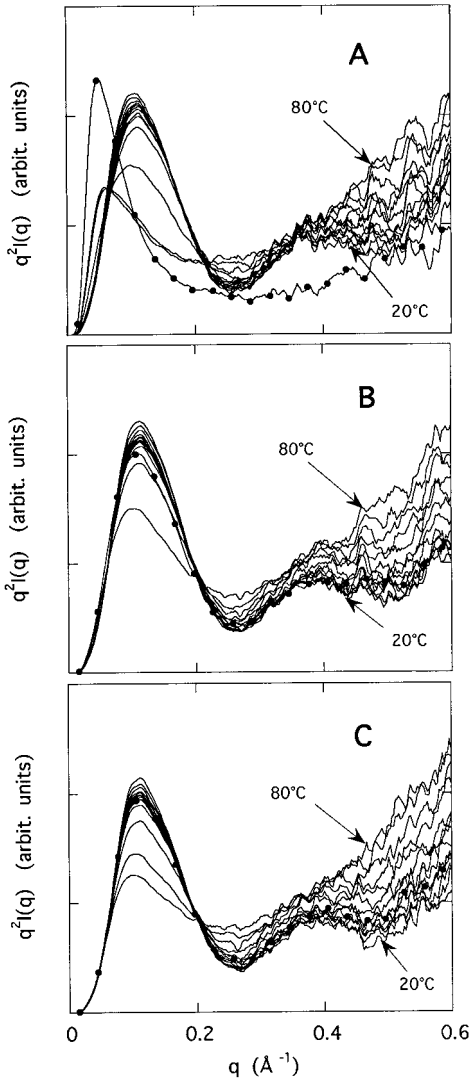

FIGURE 3 Temperature dependence of the Kratky plots ($q^2 \times I(q)$ vs. q plots) of the scattering curves in Fig. 2. *A*, *B*, and *C* and the solid lines with ● are as in Fig. 2.

proteins hold compact structures because the position and height of the peak mostly reflect the dimension and compactness of the tertiary structure of the protein (Kataoka et al., 1995; Kataoka and Goto, 1996). In comparison with the gradual changes of the Kratky plots in the q range of 0.4–0.6 $Å^{-1}$, the peaks at $q \approx 0.12$ $Å^{-1}$ in Fig. 3 change drastically at higher temperatures for all pH values. The above changing tendencies both in the scattering curve and in the Kratky plot at the different q ranges strongly suggest that the intramolecular structural change proceeds gradually, such as a second-order transition, and that the tertiary structural change occurs such as a first-order transition. We can also recognize an evident pH dependence of the changing tendency of the Kratky plot in the q range of 0.1–0.6 $Å^{-1}$. At pH 7.2 and 4.8, the change of the broad peak at $q \approx 0.12$ $Å^{-1}$ occurs drastically in comparison with that at pH 2.8. Especially at pH 7.2 the large shift of the peak position occurs at a temperature between 70°C and 75°C, suggesting that the thermal denaturation of lysozyme accompanies an aggregation at pH 7.2, which makes the thermal structural transition irreversible. In the scattering curve and the Kratky plot the thermal reversibility above $q \approx 0.3$ $Å^{-1}$ is higher than that below $q \approx 0.15$ $Å^{-1}$, suggesting that the intramolecular structural change is essentially reversible below pH 4.8 under the present conditions.

Fig. 4 shows the distance distribution functions $p(r)$ calculated by the Fourier transform of the scattering curves at pH 2.8 and 7.2 in Fig. 2. The variation of the $p(r)$ profile depending on temperature well reflects the thermal change of the tertiary structure. Clearly, the structural change is highly reversible at pH 2.8, whereas at pH 7.2 the structural change is remarkably irreversible owing to the aggregation. Fig. 5 shows the temperature dependence of the radius of gyration R_g obtained by using Eq. 5. In Fig. 5 the R_g begins to increase from ~65°C at pH 2.8 and 7.2 and from ~70°C at pH 4.8. The increment of the R_g value by elevating temperature from 20°C to 80°C is from 16.2 Å to 19.8 Å at pH 2.8 and from 16.3 Å to 19.5 Å at pH 4.8, indicating the expansion of the tertiary structural dimension. At pH 7.2 the remarkable increase of the R_g from 16.4 Å to 26.9 Å results from the aggregation in the thermal denaturation process, which is also shown by the drastic increase of the maximal diameter D_{max} estimated from Fig. 4.

As shown in Figs. 2, 3, and 4, the reversibility of the thermal structural transition mostly holds at low pH, especially at pH 2.8. To compare the SAXS results with the DSC ones, it is important to carry out the DSC measurements under the same solution condition of the SAXS measurements. In Fig. 6 the thermograms of the first and second heating scans at pH 7.2 and 2.8 are shown. The reversibilities of the thermal structural change shown in Figs. 2 and 3 are in good agreements with those observed in the DSC thermograms in Fig. 6. The onset and midpoint temperatures observed in the DSC thermograms are 64°C and 73°C at pH 2.8, 70°C and 77°C at pH 4.8, and 66°C and 73°C at pH 7.2, respectively. These values mostly agree with the temperatures where the significant changes of the tertiary structures were observed by the SAXS measurements in Figs. 2, 3, and 4. The decrement of the transition enthalpy of the second heating scan compared with that of the first heating one is ~25% at pH 7.2 and below 1.3% at pH 4.8 and 2.8.

The present results clearly indicate that the tertiary structural change accompanies a large heat absorption, whereas that the intramolecular structural change, namely, the pretransition observed in the q ranges of 0.3–0.6 $Å^{-1}$ starts

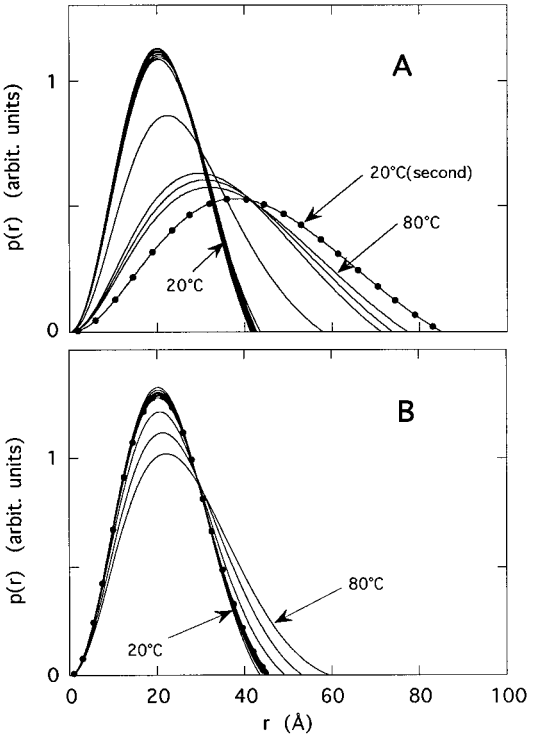

FIGURE 4 Distance distribution functions $p(r)$ calculated by the Fourier inversion of the scattering curves in Fig. 2. (*A*) pH 7.2; (*B*) pH 2.8. The solid lines with ● are as in Fig. 2.

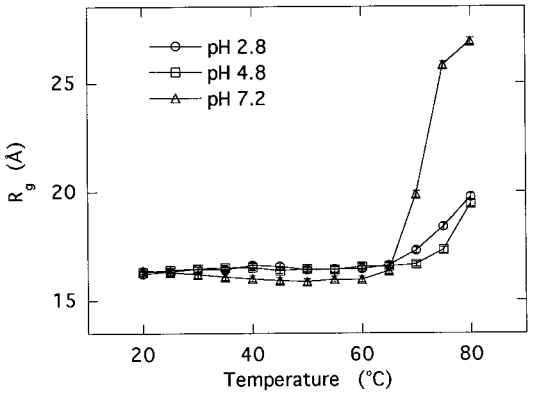

FIGURE 5 Temperature dependence of the radius of gyration R_g of the HEWL solutions (5% w/v) at different pH values. R_g values were estimated from the distance distribution functions by using Eq. 4 to the $p(r)$ functions in Fig. 4.

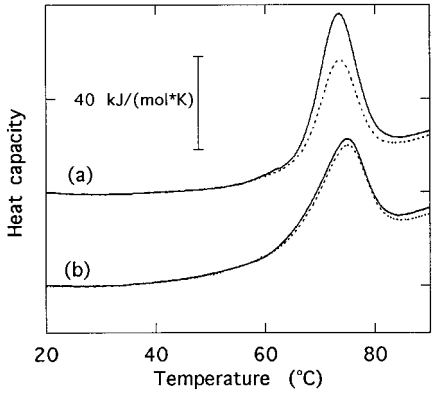

FIGURE 6 Differential scanning calorimetry thermograms of the HEWL solutions (5% w/v) at different pH values: ——— and ···, first and second heating scans, respectively. (*a*) pH 7.2; (*b*) pH 2.8. These solutions were prepared in the same way as those used for the scattering measurements in Fig. 2. The scanning rate was 3°C/min.

mostly without a heat absorption before the above main transition. These results agree with our recent paper treating the thermal structural transition of HEWL under the different solvent conditions, where we also compared the thermal structural transition process of HEWL with that of α-lactalbumin (Hirai et al., 1998). Such differences between the tertiary and intramolecular structural changes suggest that the multiplicity of the thermal transition of HEWL strongly depends on the structural hierarchy and stability, which would agree with the evidence of the multiple pathways in folding observed in two distinct folding domains of lysozyme (Miranker et al., 1991; Radford et al., 1992a,b; Buck et al., 1993). In other words, in the case of HEWL the thermal transition of the tertiary structure accompanies the thermodynamic-microstate transition with a significant change of Gibbs free energy, and the transition of the intramolecular conformation in the polypeptide chain arrangements proceeds without or with a minor change of Gibbs free energy such as a second-order transition. In addition, the structural transition feature would strongly couple the thermal stabilities of distinct folding domains, such as α and β domains, as suggested by the pH dependence of the intramolecular structural change. The above results agree with the thermodynamic consideration that the collapse of the tertiary structure would induce a significant change of the water-accessible area of the protein surface between the native state and the denatured state, resulting in changes of hydration of amino acid residues upon heating that accompany changes of heat capacity (Privalov and Makhatadze, 1990). Under theoretical bases of thermodynamics, the advanced algorithms for the analysis of DSC curves (Filimonov et al., 1982; Kidokoro and Wada, 1987; Kidokoro et al., 1988) were shown to give us not only thermodynamic functions but also the fractions of the thermodynamic microstates as an ensemble of microstates at equilibrium. On the other hand, the SR-SAXS method has a great advantage to determine directly spatial-conformational states of macromolecules, although this method has been rarely applied to discuss quantitatively those states (Lattman, 1994; Kataoka and Goto, 1996) by the occurrence of aggregation in the structural transition of proteins. The reversibility of the thermal structural transition of the proteins, which was observed in the present SAXS experiments in the wide q range by preventing aggregation, would enable us to compare directly the spatial-conformational states observed by SAXS with the thermodynamic microstates observed by DSC. Accordingly, we can develop further discussion of the folding and unfolding mechanism of proteins, especially structural energetics of the molten globule state (Mark and Gunsteren, 1992; Haynie and Freire, 1993; Hilsner and Freire, 1996). A theoretical study of protein folding using the lattice Monte Carlo simulation method has shown that the folding ability of the polypeptide chain can be characterized entirely in terms of two intrinsic characteristic temperatures (Klimov and Thirumalai, 1996). One of them is the collapse transition temperature above which the chain takes an extended random coil structure; the other is the folding transition temperature below which the chain takes a folded structure. The tertiary and intramolecular structural transitions observed separately in the present experiments would correspond to the above transitions in their theoretical work. As suggested by our present and previous experiments, gradual transitions occurring in intramolecular structures would weakly depend on solvent conditions and depend on the presence of structural domains that have different inherent structural stabilities. A new method of SAXS data analysis to examine the multiplicity of the structural transition of proteins has appeared elsewhere (Hirai et al., 1999), where we have compared directly a spatial-conformational-state transition observed by SAXS with a thermodynamic-microstate transition observed by DSC. We are now continuing experiments to confirm multiplicities of thermal transitions of other proteins depending on structural hierarchy and stability.

ACKNOWLEDGMENTS

We thank the Photon Factory Program Advisory Committee for the approval of the small-angle scattering experiments (proposal 95G094 and 98G186).

REFERENCES

Buck, M., S. E. Radford, and C. M. Dobson. 1993. A partially folded state of hen egg-white lysozyme in trifluoroethanol: structural characterization and implications for protein folding. *Biochemistry* 32:669–678.

Filimonov, V. V., S. A. Potekhin, S. V. Matveev, and P. L. Privalov. 1982. Thermodynamic analysis of scanning microcalorimetric data. *Mol. Biol.* 16:435–444.

Glatter, O. 1982. Data treatment. *In* Small Angle X-Ray Scattering. O. Glatter and O. Kratky, editors. Academic Press, London. 119–196.

Haynie, D. T., and E. Freire. Structural energetics of the molten globule state. 1993. *Proteins Struct. Funct. Genet.* 16:115–140.

Hilsner, V. J., and E. Freire. 1996. Structure-based calculation of the equilibrium folding pathway of proteins: correlation with hydroexchange protection factors. *J. Mol. Biol.* 262:756–772.

Hirai, M., S. Arai, and H. Iwase. 1999. Complimentary analysis of thermal transition multiplicity of hen egg-white lysozyme at low pH using x-ray scattering and scanning calorimetry. *J. Phys. Chem. B.* 103:549–556.

Hirai, M., S. Arai, H. Iwase, and T. Takizawa. 1998. Small-angle x-ray scattering and calorimetric studies of thermal conformational change of lysozyme depending on pH. *J. Phys. Chem. B.* 102:1308–1313.

Hirai, M., S. Arai, T. Takizawa, S. Yabuki, and Y. Sano. 1997. Dynamics and phase behavior of a supermacromolecular suspension under a magnetic field studied by time-resolved x-ray scattering. *Phys. Rev. B.* 55:3490–3496.

Hirai, M., T. Hirai, and T. Ueki. 1993. Conformational change on polymer chains of partially formalized poly(vinyl alcohol)-iodine color complex studied by using synchrotron radiation small-angle x-ray solution scattering. *Makromol. Chem.* 194:2885–2895.

Hirai, M., T. Hirai, and T. Ueki. 1994. Effect of branching of amylopectin on complexation with iodine as steric hindrance. *Polymer.* 35: 2222–2225.

Hirai, M., T. Takizawa, S. Yabuki, and K. Hayashi. 1996a. Intermicellar interaction of ganglioside aggregates and structural stability. *J. Chem. Soc. Faraday Trans.* 92:4533–4540.

Hirai, M., T. Takizawa, S. Yabuki, T. Hirai, T. Ueki, and Y. Sano. 1995. Time-transient process of magnetically induced growth of nematic domains in a biological macromolecular liquid crystal. *Phys. Rev. E.* 51:1263–1267.

Hirai, M., T. Takizawa, S. Yabuki, Y. Nakata, and K. Hayashi. 1996b. Thermotropic phase behavior and stability of monosialoganglioside micelles in aqueous solution. *Biophys. J.* 70:1761–1768.

Kataoka, M., and Y. Goto. 1996. X-ray solution scattering studies of protein folding. *Folding Design.* 1:R107–R112.

Kataoka, M., I. Nishi, T. Fujisawa, T. Ueki, F. Tokunaga, and Y. Goto. 1995. Structural characterization of the molten globule and native states of apomyoglobin by solution x-ray scattering. *J. Mol. Biol.* 249: 215–228.

Kidokoro, S., H. Uedaira, and A. Wada. 1988. Determination of thermodynamic functions from scanning calorimetry data. II. For the system that includes self-dissociation/association process. *Biopolymers.* 27: 271–297.

Kidokoro, S., and A. Wada. 1987. Determination of thermodynamic functions from scanning calorimetry data. *Biopymers.* 26:213–229.

Klimov, D. K., and D. Thirumalai. 1996. Factors governing the foldability of proteins. *Proteins Struct. Funct. Genet.* 26:411–441.

Kratky, O., and G. Porod. 1949. Röntgenuntersuchung gelöster fadenmoleküle. *Recl. Trav. Chim. Pays-Bas.* 68:1106–1122.

Kriste, R. G. 1967. Neue Vorstellungen über statistische fadenknäuel. *Makromol. Chem.* 101:91–103.

Kriste, R. G., and R. C. Oberthür. 1982. Synthetic polymers in solution. *In* Small Angle X-Ray Scattering. O. Glatter and O. Kratky, editors. Academic Press, London. 387–431.

Lattman, E. E. 1994. Modeling compact denatured states of proteins. *Curr. Opin. Struct. Biol.* 4:87–92.

Mark, A. E., and W. F. Gunsteren. 1992. Simulation of the thermal denaturation of hen egg white lysozyme: trapping the molten globule state. *Biochemistry.* 31:7745–7748.

Miranker, A., S. E. Radford, M. Karplus, and C. M. Dobson. 1991. Demonstration by NMR of folding domains in lysozyme. *Nature.* 349: 633–636.

Pfeil, W., and P. L. Privalov. 1976a. Thermodynamic investigation of proteins. I. Standard functions for proteins with lysozyme as an example. *Biophys. Chem.* 4:23–32.

Pfeil, W., and P. L. Privalov. 1976b. Thermodynamic investigation of proteins. II. Calorimetric study of lysozyme denaturation by guanidine hydrochloride. *Biophys. Chem.* 4:33–40.

Pfeil, W., and P. L. Privalov. 1976c. Thermodynamic investigation of proteins. III. Thermodynamic description of lysozyme. *Biophys. Chem.* 4:41–50.

Privalov, P. L. 1989. Thermodynamic problems of protein structure. *Annu. Rev. Biophys. Chem.* 18:47–69.

Privalov, P. L., and S. J. Gill. 1988. Stability of protein structure and hydrophobic interaction. *Adv. Protein Chem.* 39:191–234.

Privalov, P. L., and G. I. Makhatadze. 1990. Heat capacity of proteins. II. Partial molar heat capacity of the unfolded polypeptide chain of proteins: protein unfolding effects. *J. Mol. Biol.* 213:385–391.

Radford, S. E., M. Buch, K. D. Topping, C. M. Dobson, and P. A. Evans. 1992a. Hydrogen exchange in native and denatured states of hen egg-white lysozyme. *Proteins Struct. Funct. Genet.* 14:237–248.

Radford, S. E., C. M. Dobson, and P. A. Evans. 1992b. The folding of hen lysozyme involves partially structured intermediates and multiple pathways. *Nature.* 358:302–307.

Tanford, C. 1968. Protein denaturation. *Adv. Protein Chem.* 23:121–282.

Tanford, C. 1970. Protein denaturation. *Adv. Protein Chem.* 24:1–95.

Ueki, T., Y. Hiragi, M. Kataoka, Y. Inoko, Y. Amemiya, Y. Izumi, H. Tagawa, and Y. Muroga. 1985. Aggregation of bovine serum albumin upon cleavage of its disulfide bonds, studied by the time-resolved small-angle x-ray scattering technique with synchrotron radiation. *Biophys. Chem.* 23:115–124.